LUT-YLIOPISTO
LUT School of Energy Systems
LUT Kone
BK10A0402 Kandidaatintyö

CHARACTERIZATION OF HEAT EFFECTS ON DEFORMATIONS OCCURRING DURING METAL L-PBF BASED ON SIMULATION

METALLIEN LASERPOHJAISESSA JAUHEPETISULATUKSESSA LÄMPÖVAIKUTUKSESTA JOHTUVIEN MUODONMUUTOSTEN KARAKTERSOINTI SIMULOINNILLA

Lappeenrannassa 16.06.2020
Sami Westman
Tarkastaja Professori Heidi Piili, TkT
Ohjaaja Projektitutkija Niko Riikonen, DI

TIIVISTELMÄ

LUT-YLIOPISTO
LUT Energiajärjestelmät
LUT Kone

Sami Westman

Metallien laserpohjaisessa jauhepetisulatuksessa lämpövaikutuksesta johtuvien muodonmuutosten karakterisointi simuloinnilla

Kandidaatintyö

2020

47 sivua, 30 kuvaa, 7 taulukkoa ja 1 liite

Tarkastaja: Professori Heidi Piili, TkT

Ohjaaja: Projektitutkija Niko Riikonen, DI

Hakusanat: Jauhepetisulatus, L-PBF, AM, 3D-tulostus, metalli, simulaatio, muodonmuutos, jäännösjännitys

Tämän kandidaatin työn tarkoituksena oli selvittää jauhepetisulatuksen aikana osassa esiintyviä lämmönvaikutuksia. Näitä muodonmuutoksia ja jännityksiä tutkittiin simulaation avulla. Tutkimuksen avulla voitaisiin vähentää tulostuksen aikana tapahtuvia ongelmia ennen oikeaa tulostusta. Työssä simulaation parametreinä käytettiin EOS M290 jauhepeti tulostimen parametrejä nikkelipohjaiselle työkaluteräkselle (MS1) materiaalin tulostukseen. Materiaaliksi valittiin MS1, sillä sitä on LUT Laser tutkimus ryhmällä käytössä.

Kirjallisuuskatsauksen perusteella hankalimpia geometrioita tulostaa ovat ulokkeet ilman tukirakenteita ja ohuet vaakatason levyrakenteet. Ulokkeisiin kertyy ylimääräistä lämpöä, sillä lämpö johtuu huonommin jauheeseen kuin tukirakenteisiin. Tämä johtaa jauheen osittaiseen sulamiseen. Vaakatason ohuet rakenteet pyrkivät taipumaan ylöspäin reunoista lämpölaajenemisen seurauksena. Tämä voidaan välttää kappaleen orientaatiolla.

Simulaatioissa huomattiin, että kaikkien rakenteiden pääasiallinen muodonmuutos oli kutistumista. Kun materiaalia sulatetaan, tapahtuu siinä lämpölaajenemista. Kutistuminen tapahtuu, kun materiaali vetäytyy jäähtyessään. Jännitykset syntyvät näistä muutoksista. Suurin osa kappaleiden jäännösjännityksistä muodostui kappaleiden pinnalle. Vaikka materiaalin myötölujuuden ylittäminen on edellytys muodonmuutokselle, ei se välttämättä johda muodon muutokseen. Kappaleiden ja rakennus alustan rajapinnalla jännitykset olivat korkeimpia, mutta muodonmuutokset olivat pieniä. Rakennus alustan tuki esti muodonmuutokset

Jatkossa olisi syytä tutkia kappaleen irrotuksen ja lämpökäsittelyn vaikutuksia muodonmuutoksiin, sillä niiden vaikutukset voivat olla suuria. Lisäksi tarkastelun kohteena voisi olla eri simulaatio tapojen tuloksien eroja tehokkaimman metodin ja niiden erojen selvittämiseksi.

ABSTRACT

LUT University
LUT School of Energy Systems
LUT Mechanical Engineering

Sami Westman

Characterization of heat effects on deformations occurring during the L-PBF based on simulation

Bachelor's thesis

2020

47 pages, 30 figures, 7 tables and 1 appendix

Examiner: Professor Heidi Piili

Supervisor: M. Sc. (Tech.) Niko Riikonen

Keywords: L-PBF, simulation, metal, deformation, residual stress, 3D-printing, AM, Thermo-mechanical

The purpose of this bachelor's thesis was to determine the heat effects that occur in the part during powder bed fusion process. These deformations and residual stresses were investigated by using simulation. The study could help reduce problems that occur during printing before the actual printing. The parameters for nickel-based tool steel (MS1) on EOS M290 was used as parameters for the simulation. MS1 was chosen as the material because it has been used by the LUT Laser Research Group.

Difficult geometries for printing are overhang without supporting structures and thin horizontal plate structures based on the literature review. The overhangs accumulate extra heat, as raw powder has worse heat conductivity than solid support structures. This leads to partial melting of the powder at the surface. The thin structures of the horizontal tend to bend upwards from the edges as a result of thermal expansion. This can be avoided with orientation of the part.

The simulations found that the main deformation of all structures was shrinkage. When the material is melted, thermal expansion occurs. Shrinkage occurs when the material contracts when it cools down. The tensions form from these changes. Most of the residual stresses in the pieces consisted of the surface of the pieces. Although exceeding the yield strength of the material is a prerequisite for deformation, it does not necessarily lead to a change of shape. The objects and building the chassis interface had the highest stresses, but the deformations were minimal. Building chassis support prevented deformation.

In the future, it would be necessary to examine the effects of the removal and heat treatment of the body on the deformation, as their effects can be large. In addition, the results of the different simulation methods could be considered to determine the most effective method and their differences.

ACKNOWLEDGEMENTS

This study was carried out as part of Metal 3D Innovations (Me3DI) project funded by European Regional Development Fund (ERDF). Aim of this project is to form knowhow cluster for metal 3D printing to South Karelia. Project started 1.9.2018 and it ends 31.12.2020. Thesis was produced in Research Group of Laser Material Processing and Additive Manufacturing (3D Printing) of Department of Mechanical Engineering at LUT University

I would like to thank Professor Heidi Piili and supervisor Niko Riikonen from helping me through this thesis.

I would also like to thank whole staff of Research Group of Laser Material Processing and Additive Manufacturing (3D Printing) at LUT University.

Sami Westman

Sami Westman

Lappeenranta 2020

LIST OF CONTENTS

TIIVISTELMÄ

ABSTRACT

ACKNOWLEDGEMENTS

TABLE OF CONTENTS

LIST OF SYMBOLS AND ABBREVIATIONS

1 INTRODUCTION 8

1.1 Motivation, research problem and research questions 8

1.2 Objective 8

1.3 Scope 9

1.4 Industrial Relevance 9

2 METHODS 10

2.1 Literature review 10

2.2 Simulation 10

2.3 Interview 11

3 LITERATURE REVIEW 12

3.1 Thermo-mechanical method 12

3.2 Coupled and decoupled models 16

3.3 Finite element method 17

3.4 Challenging geometries for L-PBF 18

3.5 Using simulation to mitigate distortion 21

3.6 Tool steel of MS1 22

4 SIMULATIONS 24

4.1 Powder bed fabrication application 26

4.2 Additive Manufacturing scenario App 30

5 RESULTS AND DISCUSSION 33

5.1 Overhang 33
5.2 Arch structure 36
5.3 Horizontal plate 39
5.4 Discussions 40
6 CONCLUSIONS 42
7 FURTHER STUDIES 44
LIST OF REFERENCES 45
APPENDIX

LIST OF SYMBOLS AND ABBREVIATIONS

2D	Two-dimensional
3D	Three-dimensional
AM	Additive manufacturing
CAD	Computer aided design
FEM	Finite element method
ESPI	Electronic speckle pattern interferometry
L-PBF	Laser powder bed fusion
PBF	Powder bed fusion

1 INTRODUCTION

Laser powder bed fusion (L-PBF) is an additive manufacturing (AM) method suitable for manufacturing metal parts. In L-PBF, the raw material is in powder form and the metal powder is layered and then melted, usually with laser beam, to form a layer of the printed object. The building platform is lowered and new layer of powder is spread and melted. This process is repeated until object is ready. (Acharya et al. 2016, pp 360-362).

This study was carried out as part of Metal 3D Innovations (Me3DI) project funded by European Regional Development Fund (ERDF). Aim of this project is to form knowhow cluster for metal 3D printing to South Karelia. Project started 1.9.2018 and it ends 31.12.2020. Thesis was produced in Research Group of Laser Material Processing and Additive Manufacturing (3D Printing) of Department of Mechanical Engineering at LUT University

1.1 Motivation, research problem and research questions

Laser beam used in the process heats the powder to the melting point which creates residual stresses in the object when it cools and solidifies. These stresses may cause deformations and weaken the structure and this way in worst case make the part unusable. Certain geometries are more prone to deformations. Testing these geometries experimentally is resource and time intensive. The behavior of test pieces can be evaluated using advanced computer software to save resources. (Gouge & Michaleris 2018, p. 3.; Acharya et al. 2016, pp. 360-362.)

Research questions are of this thesis are:

- What effects heat has on printed part
- What geometries cause distortion?
- Why certain geometries cause distortion?
- What can be done to decrease the distortions?

1.2 Objective

Objective of this thesis is to identify problematic geometries in L-PBF and study how to modify them to avoid these problems while maintaining the functionality. It is possible to

modify the object, optimize the parameters and build orientation to improve the build quality and efficiency before actual test prints with simulation of the AM process. Optimized process will require less test prints and save material and time. Faulty print may also push the build onto next layer, thus impairing movement of recoater blade. (Gouge & Michaleris 2018, p. 3.)

1.3 Scope

As a manufacturing method, AM is still relatively new and it develops rapidly. This makes research to become outdated fast. To ensure the quality of the literature sources, only references published after 2015 are used in this thesis. Since simulation process is time-consuming, only a few models are simulated in this study using thermo-mechanical method for L-PBF. The simulations are performed with EOS M290 parameters for EOS tool steel MS1. Simulated parts are similar to parts in literature review studies.

1.4 Industrial Relevance

AM is expensive process. Many test products have to be printed when designing AM product. These tests consume a lot of resources and time and have a possibility to break the machine. Simulation of the process would mitigate risks and save time and resources. Simulation could make stacking (manufacturing multiple parts at the same time) easier.

2 METHODS

Literature review of the study was conducted using sources from LUT Finna and Google Scholar. Simulation is run on Dassault Systèmes 3D-Experience platform, which is platform that provides applications from 3D modelling to marketing. Models used in simulations were created using 3DExperiece and Solidworks.

2.1 Literature review

Literature review was conducted to study how thermo-mechanical analysis works is theory and what things it has to take into account for accurate simulation. Tensile test for nickel-based tool steel MS1 is used to acquire yield strength of MS1.

Publications of test prints of different geometries found from literature are studied in this thesis. Test results were used to verify the simulations. Geometries that cause problems are chosen from these publications and tests executed in these as models for the simulation part. self-development of geometries would make the thesis too broad Results are required for these geometries to compare to simulation results. Review also contains an example study where simulations has been used to get better results of prints.

2.2 Simulation

The simulations were performed with 3DExperience which is "*business experience platform*" (Dassault Systèmes 2020) made by Dassault Systèmes. It is a platform that provides different kinds of applications for different uses from mechanics to marketing. Applications used in study are shown in figure 1.

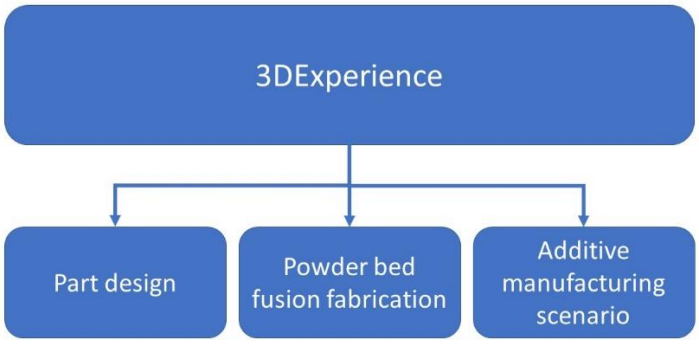

Figure 1. Applications of simulation software of 3DExperience used in this thesis.

Figure 1 illustrates three applications used in this thesis. These applications are part of 3DExperiece platform. Part designer is 3D modeling application which is similar to Dassault Systèmes Solidworks. Powder bed fabrication application is used to define L-PBF process. It allows to set the settings for the printing process, such as scan speed, laser power, scan path of laser beam and the placement and orientation of the part, including the support structures. This process can then be sent to AM device for printing or move to the next application for simulation. Simulations are done in the additive manufacturing scenario (AM scenario) application. AM scenario uses defined process from PBF fabrication to simulate it. 3D models of the part, support structures and build platform are also meshed in AM scenario. Meshing is explained in chapter 4.2. The application also requires defining of the material of the part and other parameters to simulate real AM process. (Dassault Systèmes 2020)

2.3 Interview

Simulation results are verified using knowledge of research group of Laser material processing and additive manufacturing of LUT University. This verification is executed by Heidi Piili. Reason for verification is to make sure the simulation results reflect reality. Writing error in simulation parameters may cause error in results.

3 LITERATURE REVIEW

Additive manufacturing process is time taking and expensive. Mitigating failures before the actual printing, can save money and time. It is possible to analyze heat flow and mechanical deformations during the process using simulation. These analyses can be used to predict the thermal and mechanical behavior of the part and optimize the process. (Diegel et al. 2019, pp. 76–77; Milweski 2017, pp. 105–106; Bugatti & Semeraro 2018, pp. 329-330.)

Simulating AM process is complicated process with a lot of variables. Simulating real life process demands considerable amount of computational power and may take longer than the actual process. Different methods have been invented to achieve reasonable simulation times. One of the methods is thermo-mechanical analysis. (Bugatti & Semeraro 2018, pp. 330-331; Gouge et al. 2019, pp. 1–2.). Thermo-mechanical is explained in chapter 3.1.

3.1 Thermo-mechanical method

Thermo-mechanical method is a type of simulation used for simulating additive manufacturing process. Two models are created in this process. Thermal history of printed part is calculated in thermal model. Mechanical model uses the data from thermal model to calculate stresses and distortions caused by the changes in temperature. Simulation of additive manufacturing is a complicated process requiring a lot of specific parameters to achieve accurate results. (Gouge & Michael 2018, pp. 21, 25-26.)

Material is added to build the part in additive manufacturing. This addition of material have to be simulated with new equations that come with it. There are two methods of doing this which are 1) quiet method and 2) dead-alive method. (Gouge & Michael 2018, pp. 10, 27-28.). Quiet method is illustrated in figure 2.

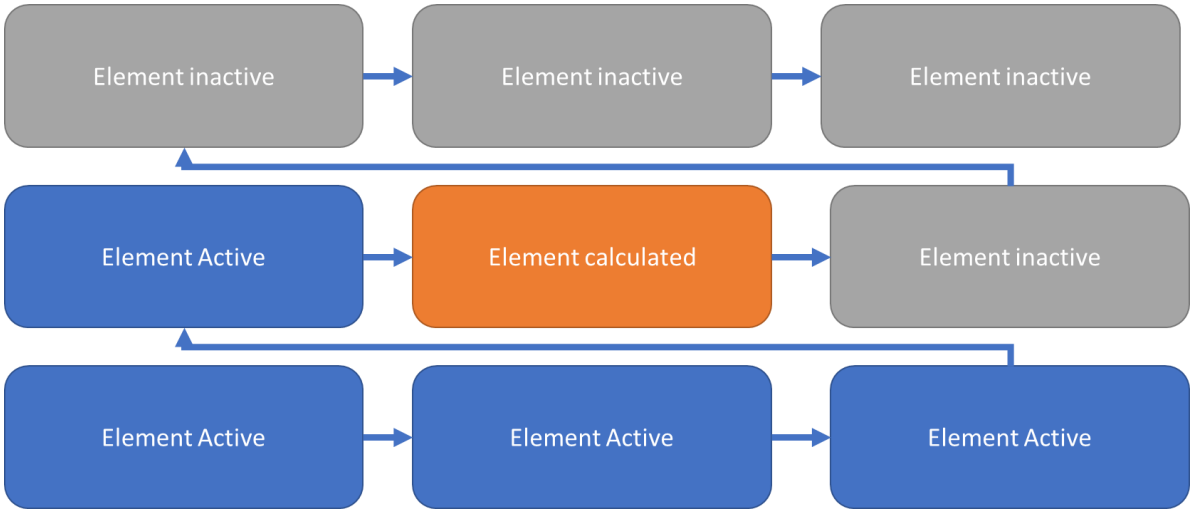

Figure 2. Quiet methods lowers inactive elements properties before activation.

Figure 2 shows that the quiet method has all the elements and equations in the model from the beginning, however their properties (such as thermal conductivity) have been set low to not affect the analysis before activation. Material is added using scaling factors. (Gouge & Michael 2018, pp. 10, 27-28.). Dead-alive method shown in figure 3.

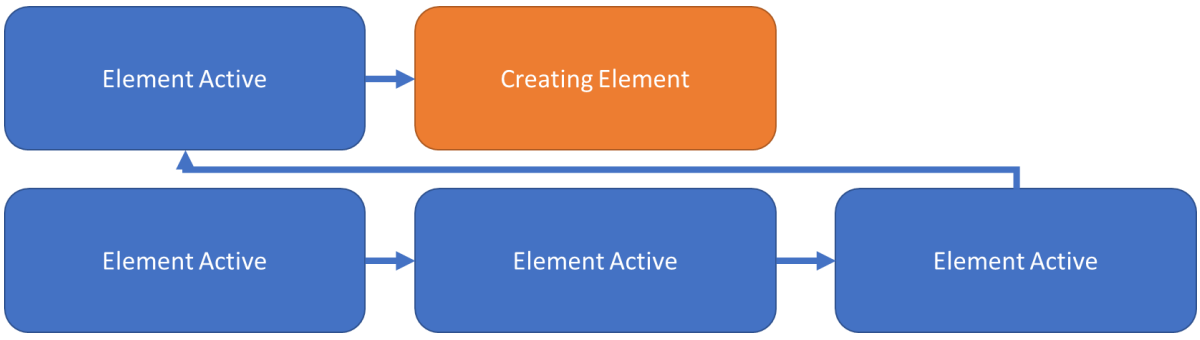

Figure 3. Dead-alive method "deletes" inactive elements and creates the upon activation.

As seen in figure 3 dead-alive method removes inactive elements before simulation. Elements are created upon their activation. (Gouge & Michael 2018, p. 10, 27-28.)

Heat source is a fundamental part of AM. By melting the powder, the part is produced. It is hard to accurately simulate the heat source in simulation which is laser beam in this study.

Laser beam, size and shape of the energy input have to be taken into account as well as the amount of heat absorbed by the part to achieve accurate simulation this is shown in figure 4.

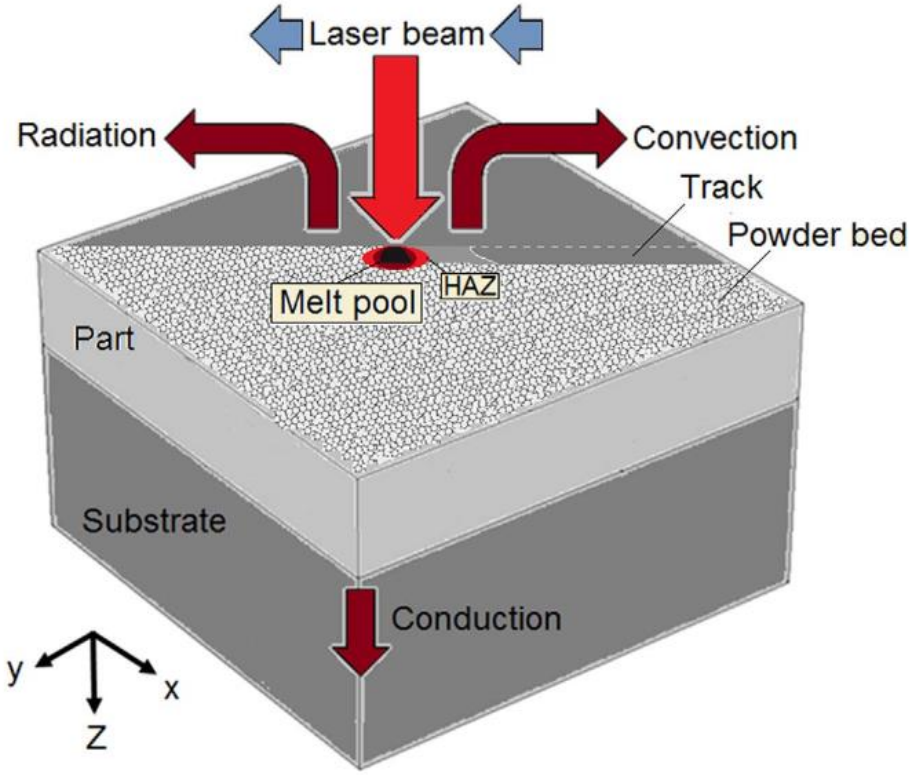

Figure 4. Some of the absorbed of laser beam energy dissipates with radiation and convection in L-PBF (Masoomi et al. 2017, p.74.)

As seen in figure 4 energy of laser beam is imputed to melt pool. Metals smooth surface reflects some of energy and this way prevents part from absorbing all of the laser beam energy. This effect is defined with absorption parameter. Energies that have been absorbed are reduced by heat convection and thermal radiation. (Gouge & Michael 2018, p. 10-11; Yang et al. 2018, p. 601.)

Material properties such as yield strength, elongation and ultimate tensile strength vary at different temperatures. Accurate thermal model is required to use these properties. Properties such as thermal conductivity, specific heat capacity, density and emissivity affect the temperatures in the part and are a source of non-linearity in thermal model. Parameters change how heat moves in the part. These properties need to be balanced with the duration of the simulation. Some of the parameters affect the results more than others. The duration of the simulation can be reduced significantly with elimination of few of thermal dependent

parameters, while keeping the ones that affect results the most gets accurate enough results. (Gouge & Michael 2018, p.12,22-23,28-29)

Heating the powder and the part with high energy creates large thermal gradients. Fast temperature increase causes thermal expansion. The material will start to shrink after the laser beam has passed and it cools down. (Peng et al 2018, pp. 871-872.). Large temperature differences result large amounts of stresses which usually exceed the yield strength of the material. These stresses may distort the product, even beyond specified tolerances making the product out of specifications. Some of the stresses can be reduced by heat treatment but excessive distortions cannot be returned to the intended shape. (Gouge & Michael 2018, p.11.)

Melting powder and cooling it down for solidification changes its microstructure of material. Microstructure of additively manufactured part depends on the rate of solidification Solidification is shown in figure 5.

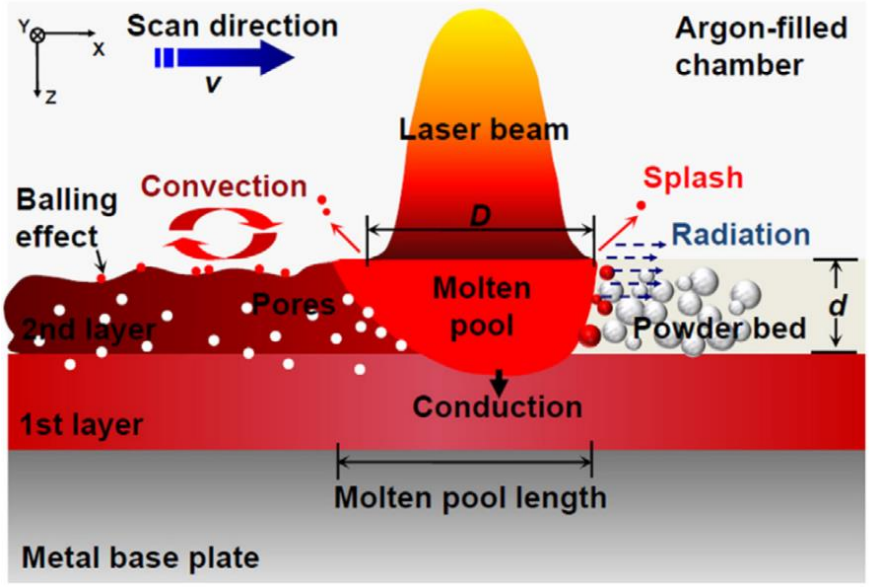

Figure 5. Formation of pores during L-PBF. (Yan et al. 2018, p. 431.)

As it can be seen in figure 5, solidified material has pores and balling. Materials properties change depending how it solidified. This means that if different areas of the printed products have different cooling rate, the material properties could also vary within the same product. (Gouge & Michael 2018, p.11; Acharya et al. 2017, p.360-362.)

3.2 Coupled and decoupled models

Thermo-mechanical simulation method have to take two phenomena into account which are mechanical and thermal responses. Conservation of thermal energy and elasto-plastic response require own equations to solve which means both need their own models. Model interaction (coupling) determines the complexity and accuracy of the complete model. (Gouge & Michael 2018, p.11-12)

Decoupled method assumes that the thermal history affects mechanical behavior, but not vice versa (Gouge & Michael 2018, p.12). Process is shown in figure 6.

Figure 6. Workflow of decoubled thermo-mechanical simulation process.

It can be seen in figure 6 that the thermal model is first simulated without taking mechanical model into account. Mechanical model is then simulated using thermal model. (Gouge & Michael 2018, p.12)

No assumptions are made in coupled method. Thermal and mechanical models are simulated simultaneously and both affect each other. Coupled method shown in figure 7.

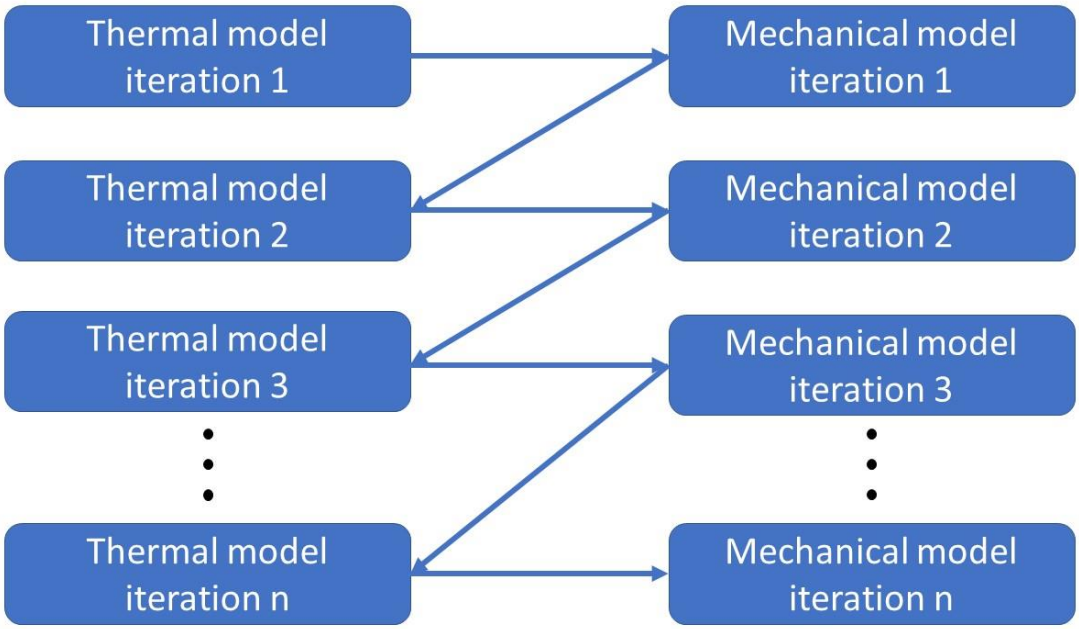

Figure 7. Workflow of coupled thermo-mechanical analysis.

Figure 7 illustrates how thermal and mechanical analyses iteration happen back to back while affecting each other. Iterations may be run multiple times to accurately take others effect into account. Temperature changes cause change in microstructure in the mechanical model. Difference in microstructure changes for example thermal conductivity in thermal model. Coupled method has more accurate results, but simulation time is longer and the load on the computer is significantly heavier. (Gouge & Michael 2018, p.12)

3.3 Finite element method

Mechanical behavior of structure is defined by differential equations. Simpler structures may be able to solve with linear using analytic method (traditional calculation methods), but more complex structures are near impossible to solve using these methods. (Neto et la. 2015, p.43)

Using FEM requires meshing of the model. Meshing means dividing the original model into finite number of elements for example squares (2D) or cubes (3D). (Neto et al. 2015, pp.46-47.). Example of mesh is shown in figure 8.

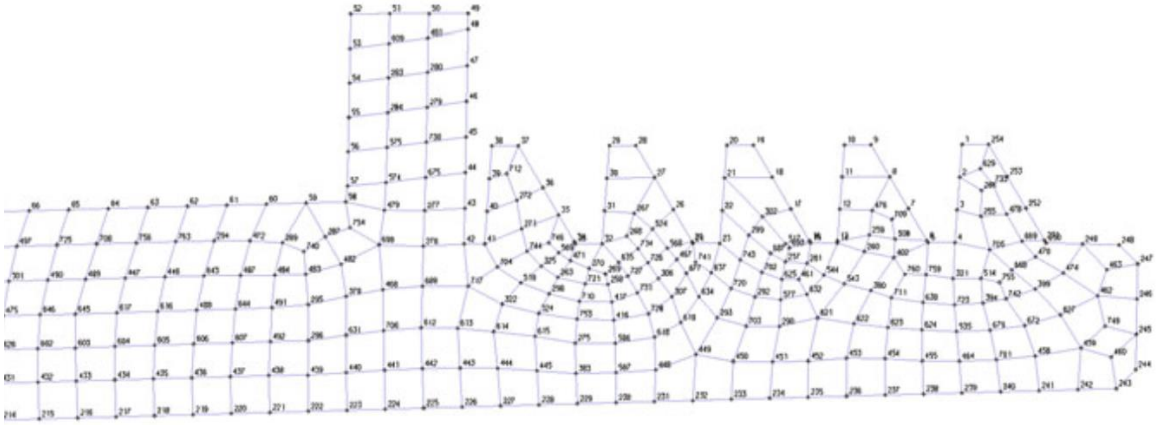

Figure 8. 2D mesh example when part is meshed for FEM (Neto et la. 2015, p.47.).

As seen in figure 8 elements are formed nodes (corners) and edges. These nodes and edges are connected to each other in such a way that it forms the original model. Different types of elements can be used in the same model as long as their connection is compatible. (Neto et al. 2015, pp.46-47.)

Each element is given coordinates local coordinates to make limit amount of variables. Elements have different equations to calculate displacements and formed stresses individually. (Neto et al. 2015, p.47-49)

3.4 Challenging geometries for L-PBF

Kokkonen et al. (2016) made a study where they designed test parts that included commonly used geometries from mechanical components. These parts were manufactured with AM and studied to find problematic geometries. (Kokkonen et al. 2016, p. 4.)

Overhanging area without support structures is challenging to manufacture by L-PBF, since melting a new layer requires support structure from the lower layer. If the lower layer does not provide enough support the melt pool is going to sink in the powder bed due to effect of gravity. Universal minimum self-supporting angle is 45°. Surfaces with inclination angle lower than 45° cannot support upper layers without support structures. (Lou et al 2019, Wang & Chou 2018). Powder has poor heat conductivity which leaves heat trapped in the overhang and melts small amounts of powder that attach to the surface. Overhangs tend to have larger melt pools compared to solid structures (Han et al. 2018). Predicted effects are represented in figure 9. (Kokkonen et al. 2016, pp. 9-12.)

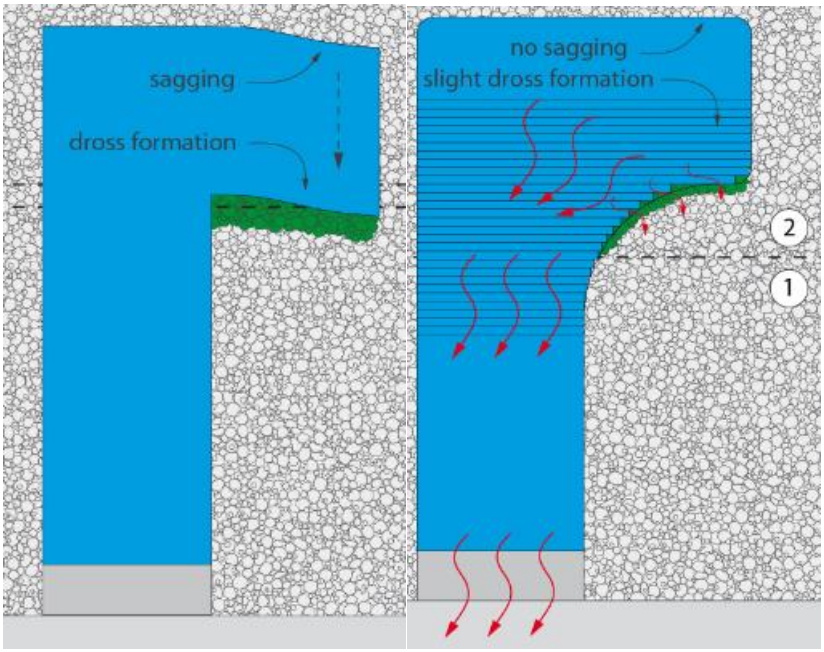

Figure 9. Overhang without support (Kokkonen et al. 2016, pp. 14-15.)

Figure 9 shows that having no support causes the overhang to sag. Dross is also formed under the overhang. Overhang could be made self-supporting by using fillet. This would give layers more support preventing sagging. Increased thermal conductivity would also decrease formation of dross. Red arrows show thermal conduction direction. Arch structure is shown in figure 10. (Kokkonen et al. 2016, pp. 14-16.)

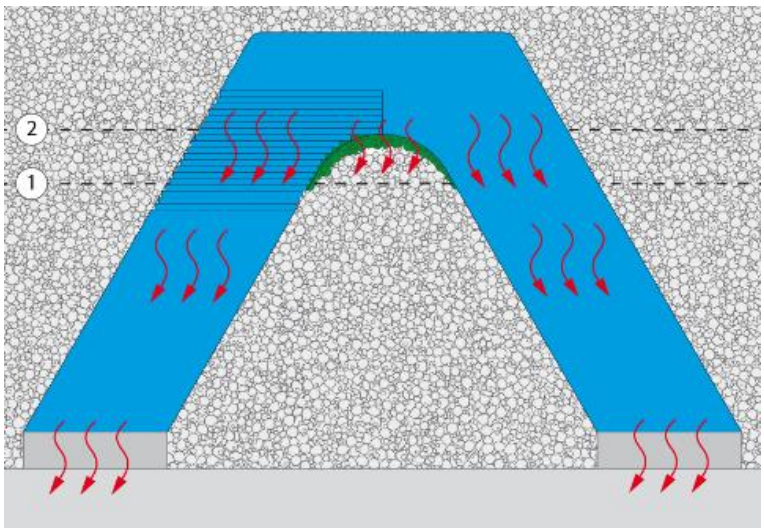

Figure 10. Arch structure (Kokkonen et al. 2016, p.13.)

Arch structure without supports (figure 10) builds up heat similarly to overhang and could lead to partial melting of the powder. Heat buildup depends on the width and angle of the

fillet, since the heat tries to transfer mainly downwards. Wide arch has large amounts of area above the powder making it the only way for the heat to transfer. Arch with fillets should be self-supporting. The printing results are shown on figure 11. (Kokkonen et al. 2016, p. 13; Amal et al. 2020, pp. 3-4.)

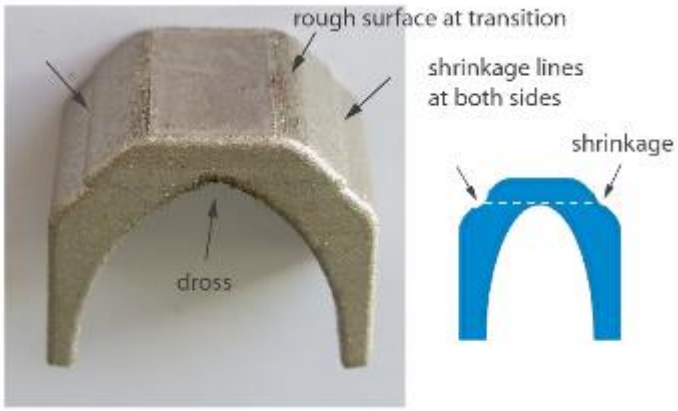

Figure 11. Arch results (Kokkonen et al. 2016, p.47.).

Figure 11 shows small amount of dross formed under the arch. In addition, it was noticed that there was traversal shrinkage at the outer side at the level where the sides meet. (Kokkonen et al. 2016, pp.46-47.)

Figure 12 illustrates surface roughness test.

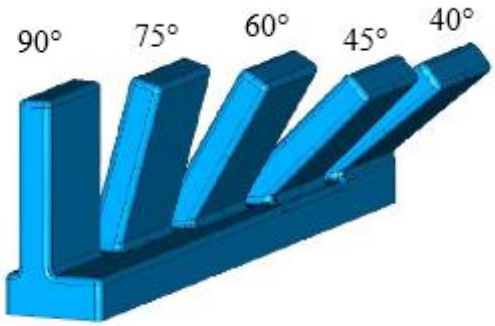

Figure 12. Angle between plates changes from 40° to 90° (Kokkonen et al. 2016, p. 29).

Figure 12 illustrates test plates used to study inclination angles effect on surface roughness. Five plates were made with angles varying from 40 degrees to 90 degrees. Small amount of sagging was noticed on 60-degree plate. Surface roughness increased with smaller angles. (Kokkonen et al. 2016, p. 29, 53-54.). In figure 13 is shown printed results.

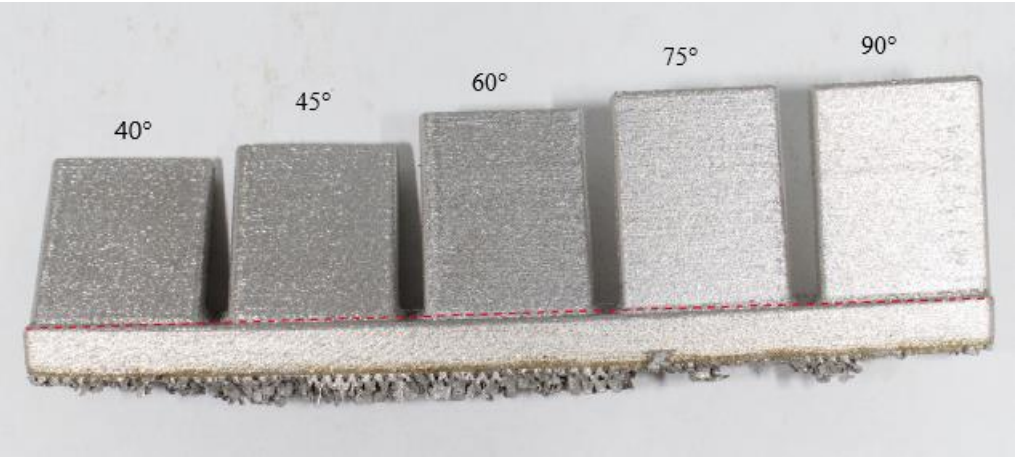

Figure 13. Print test result with bent plate manufactured with SLM125 using AlSi12 (Kokkonen et al. 2016, p. 23).

As it is shown in figure 13 thermal stresses caused the plate to bend upwards. This makes removal of the supports structures harder. Surface quality of the bottom of the plate is rough and burned.

3.5 Using simulation to mitigate distortion

Two impellers and two miniature bridges were printed from 316L using Renishaw AM250 AM device to prepare to the experiment. (Yaghi, Ayvar-Sob et al. 2019, p. 225.) Prints shown on figure 14.

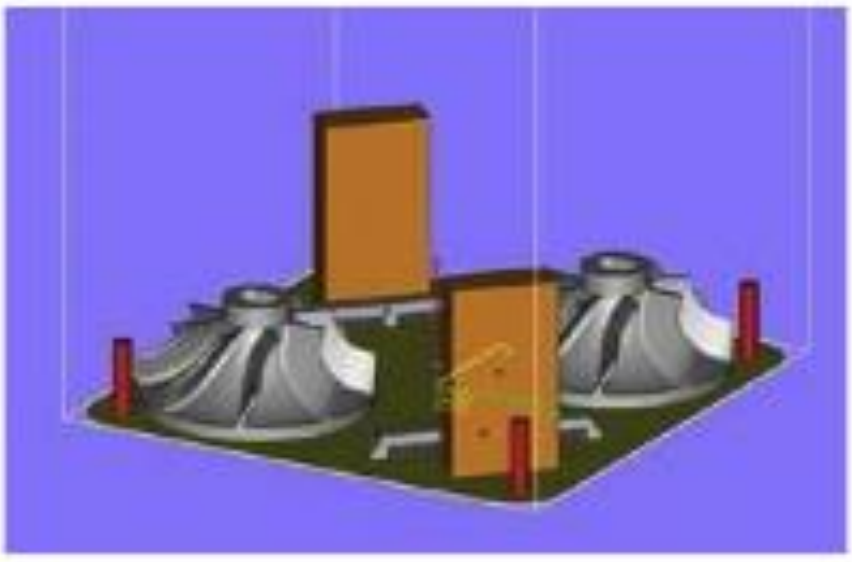

Figure 14. Print model for the test (Yaghi, Ayvar-Sob et al. 2019, p. 225.).

Figure 14 illustrates the model used in the study. Distortions were monitored using GOM ATOS triple scan optical system (Yaghi et al. 2019, pp. 225-226). Measuring points are indicated in figure 15.

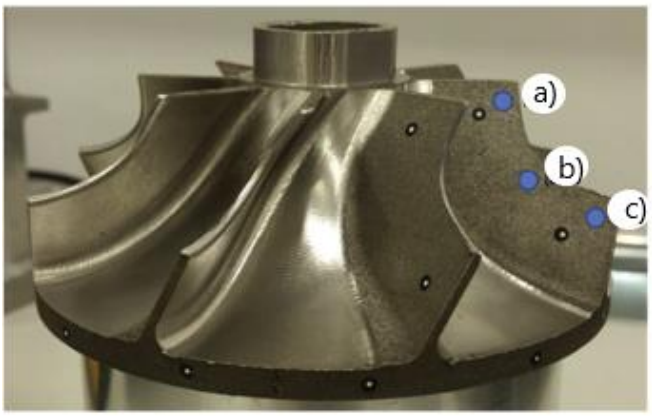

Figure 15. Impeller with measuring point a, b and c marked (Yaghi et al. 2019, p. 225-226))

Figure 15 shows measurement points for distortion. Measured distortion were 37 µm for point a, 15 µm for point b and 10 µm for point c. Impeller shown in figure 15 was used to measure residual stresses in the bottom plane. Small holes were drilled on the surface of the plane. These drillings were recorded using CCD camera to measure displacements caused by relaxation of stresses. Highest measured stress was 550 MPa which was from the closest measured point to the center. (Yaghi, et al. 2019, p. 225-226)

Simulation was conducted on impeller model using inherent strain method and using same parameters. Results of this simulation was compared to results of the two printed impellers. Stresses between simulation and print were mostly similar. Only noticeable different was lower stresses in simulation at few points. (Yaghi et al. 2019, p. 229-230)

The simulation results were reverse engineered to produce a new model where the distortions were compensated for. A new impeller was printed using the compensated model. On the new product the distortions from the desired geometry was over 50 % less than on uncompensated impeller. (Yaghi et al. 2019, pp. 233-235.)

3.6 Tool steel of MS1

Cyr, Lloyd et al. (2018) carried out a study where EOS M290 metal AM machine was used to manufacture test parts from tool steel EOS MS1 using parameters listed in see table 1.

Table 1. Printing parameters for MS1. (Cyr, Lloyd et al. 2018, p. 290.)

Print bed temperature [°C]	40
Laser Power [W]	285
Scan speed [m/s]	0.96
Layer thickness [mm]	0.04
Hatch distance [mm]	0.11

As table 1 shows AM process uses heated bed and layer thickness is quite small. These parts were used to test yield strength, ultimate tensile strength and fracture strain of MS1. Results of these test are listed in table 2. (Cyr, Lloyd et al. 2018, pp. 290-291.)

Table 2. Test results. (Cyr, Lloyd et al. 2018, p. 291.)

	Yield strength [MPa]	Ultimate tensile strength [MPa]	Fracture strain
Vertical Tension	900 MPa	1120 MPa	0.12
Horizontal Tension	1000 MPa	1225 MPa	0.135
Compression	1200 MPa	1450 MPa	0.425

As table 2 reveals that MS1 has large ultimate tensile strength. According to results MS1 has "significant anisotropy due to build direction". Material yield strength is about 100 MPa different between horizontal and vertical strength values. (Cyr, et al. 2018, pp. 293-294.) These parameters shown in table 1 are used in this thesis.

4 SIMULATIONS

Simulation for this thesis is done with thermo-mechanical method for more accurate results, but decoupled method is used to reduce the strain on computer and shorten the simulation time. Simulations were done to better understand the phenomena happening during and after the AM process. Simulation requires a lot of parameters. The most important parameters are discussed in this chapter. All the parameters are also listed in the attachments of this thesis. Part used in this thesis are also shown in this chapter.

3D model of the object is necessary for the simulations. The model can be made in 3DExperience or in another CAD software and imported to 3DExperience. This model is then moved to the Powder Bed Fabrication App. Figure 16 illustrates are models 1-3 that are used in simulations.

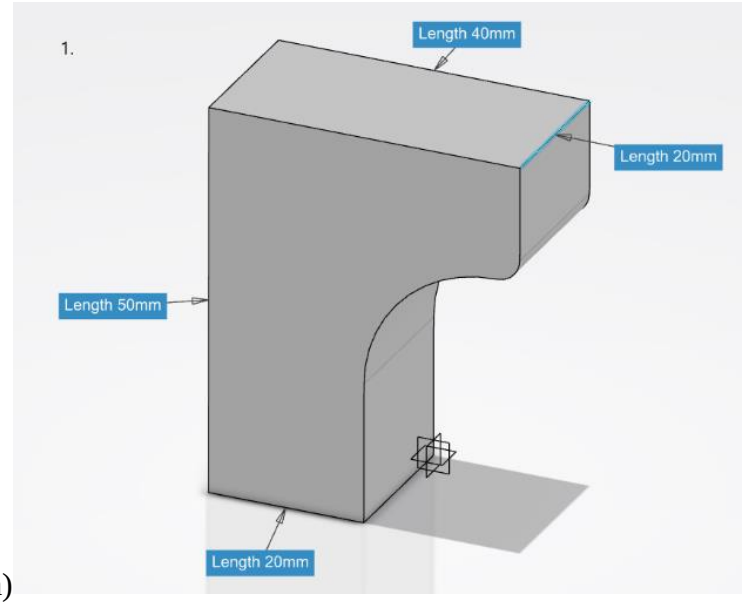

a)

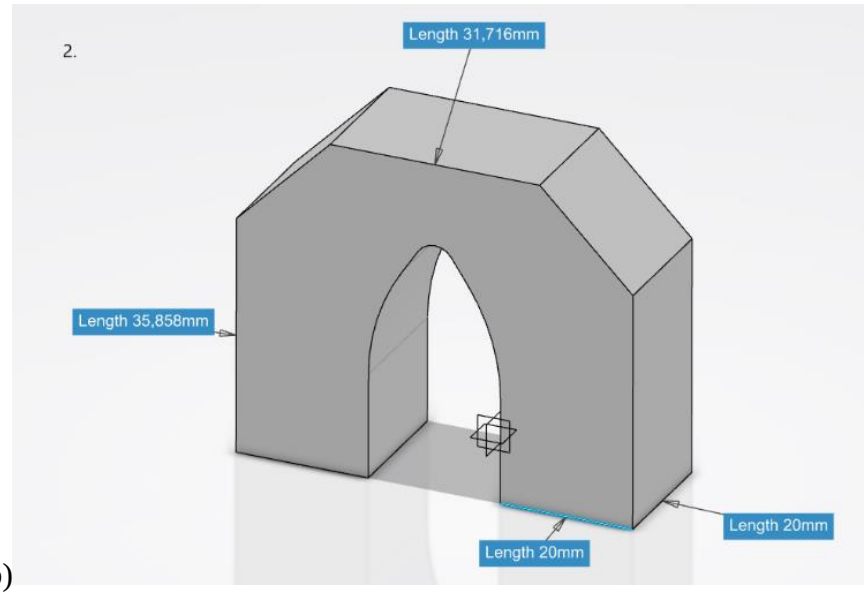

b)

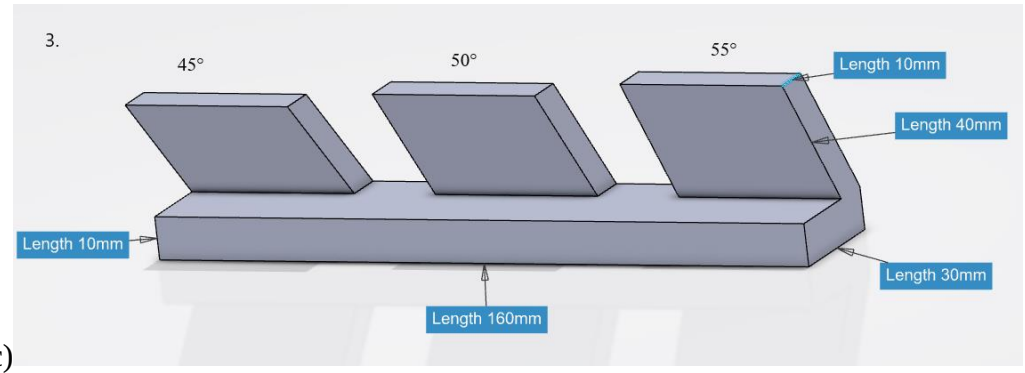

c)

Figure 16. Parts 1-3 (a.c) which are used in this thesis to further study deformations.

Models illustrated in figure 16 are similar to the ones in the study of Kokkonen et al. The height of the models is 50 mm for size reference. Parts 1 and 2 (see figure 16a and b) have

been created using 3DExperiences Part Design app and part 3 (figure 16c) with Solidworks. Part 3 does not have as many plates as the reference part. This is because the simulations do not have results for surface quality. Part 3 is used to analyze behavior of bottom plate.

4.1 Powder bed fabrication application

Powder Bed Fabrication App is used to define the parameters of the AM device such as the building chamber size, build platform size and laser parameters. Machine parameters are shown in table 3.

Table 3. EOS M290 parameters used in this study. (EOS 2019)

Construction volume [mm]	250 x 250 x 325
Max laser power [W]	400
Max scan speed [m/s]	7
Focal diameter [mm]	0.1

Parameters shown in table 3 are from EOS M290 manual. These are just maximum usable parameters so they will not affect the actual simulation. However, the build platform should be large enough, so the part easily rests on top of it.

Figure 17 shows definition of AM machine which has been defined as EOS M290

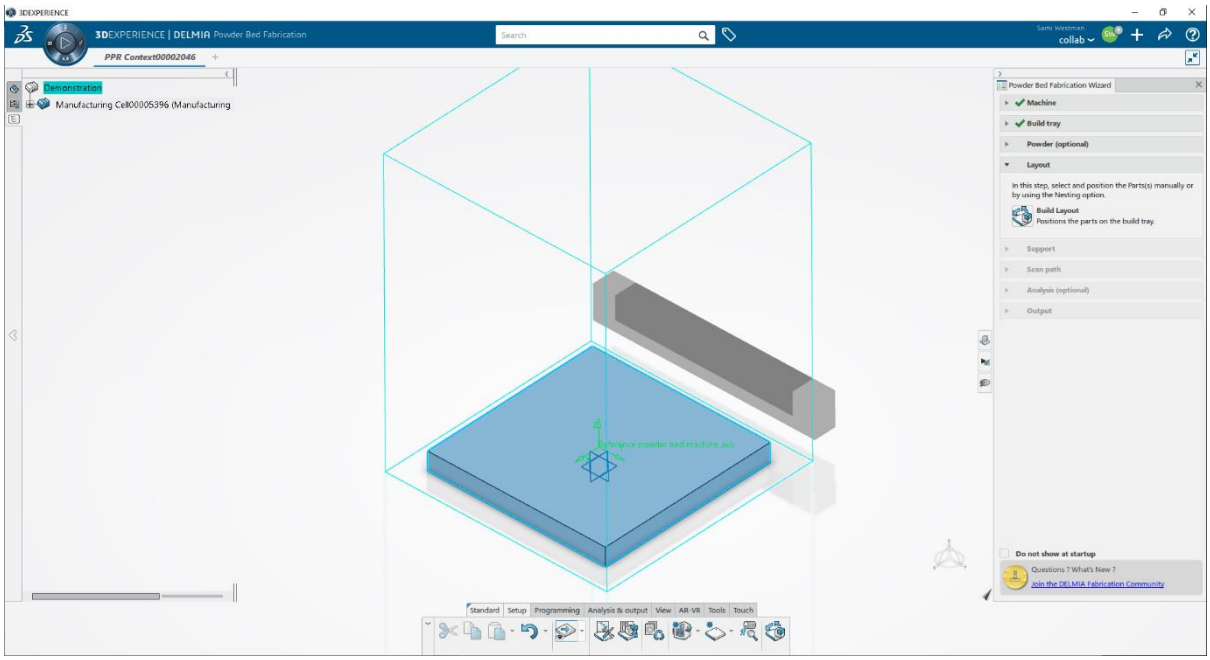

Figure 17. EOS M290 in 3DExperience

Figure 17 reveals that the build platform is smaller than construction volume. Size difference between build platform and volume does not matter as long as platform is smaller than volume. After the machine has been defined the 3D model of the part needs to be imported to the process. This can be done using build layout. If the 3D model has been saved to the 3DExperience it can be selected from the cloud. This 3D model can then be nested according to the rules and orientation. Distances of the parts are listed in table 4.

Table 4 Distances from build platform

	Distance from build platform [mm]
Part 1	0
Part 2	0
Part 3	5

Parts 1 and 2 have been set directly on build platform to avoid using supports to simplify the simulations. Part 3 was nested above the build platform to allow it to be built on supports which gives it more freedom to distort. Supports can be seen in figure 28 in chapter 5.3. In figure 18 is shown nested part 1.

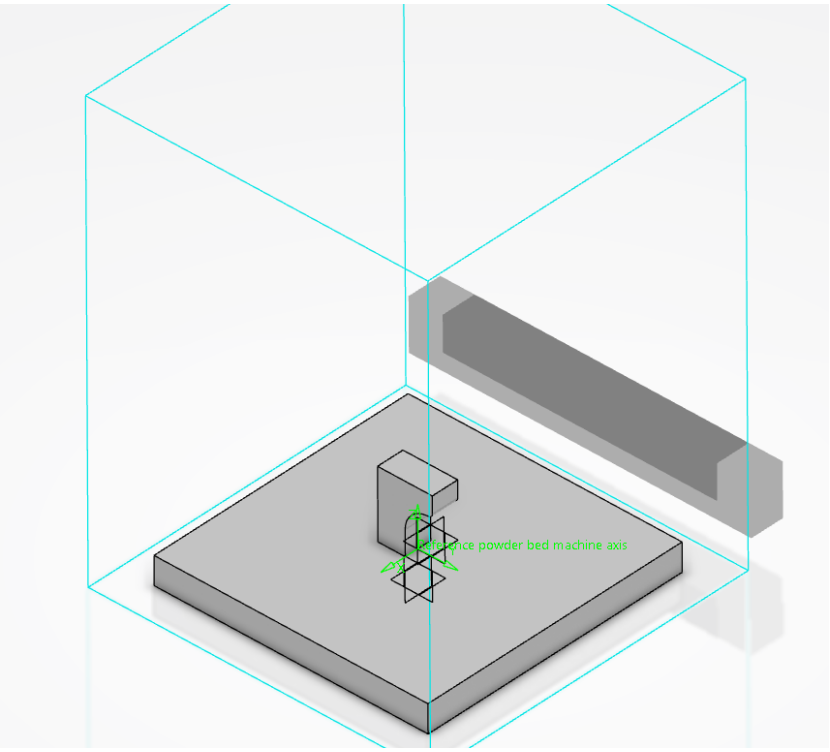

Figure 18. Nesting of part 1 in 3DExperience used in simulation of L-PBF carried out in this study.

Figure 18 reveals that part 1 has been nested directly on build platform. Part has been nested in upright position to get the overhang. Metal AM parts are usually built on support structures to make separating the part from build platform easier. Simulation in 3DExperience only supports wired support structures. These supports are created with 3 mm spacing which is higher than in actual printing but necessary to simplify the simulation. In this study, wired supports were used in grid pattern. Supports can be created manually or automatically by defining the maximum and minimum surface angle. Overhang of the part 1 has been left without support structure to maximize the distortion.

Generating a scan path of laser beam requires rules for build process, scanning and scan path. In the build process the only important parameter is recoating breaktime to give the part some time to cool down between layers. Defining starting temperature will save some simulation time later. These parameters are listed on table 5.

Table 5. Build process parameters.

Recoating breaktime [s]	7
Start temperature [K]	300

In table 5 start temperature is the temperature of the chamber temperature. This parameter itself does not do anything, but the software uses it as default temperature for later parameters.

Scanning rules are set to define the used laser power and scanning speed in the process. Process where laser is used on a surface in a "pattern" is referred as scanning. The used parameters are from study "Tension-compression asymmetry of additively manufactured Maraging steel" for EOS M 290 printing tool steel EOS MS1. Scanning rule parameters are listed in table 6.

Table 6. Scanning rules.

Beam power [W]	285
Defocusing length [mm]	0
Jump speed [m/s]	7
Delay after jump [s]	0
Scan speed [m/s]	0.96

Scanning rules are used in scan path rules to define which parameters are used for infill, contouring, upskin and downskin. In this study same parameters are used in all of them. Slicing step defines layer height. In real print a height of 0.04 mm would be used, but in this

simulation 0.1 mm is used. Using these parameters scan path of laser beam is generated. In figure 19 an example of generated scan path is represented.

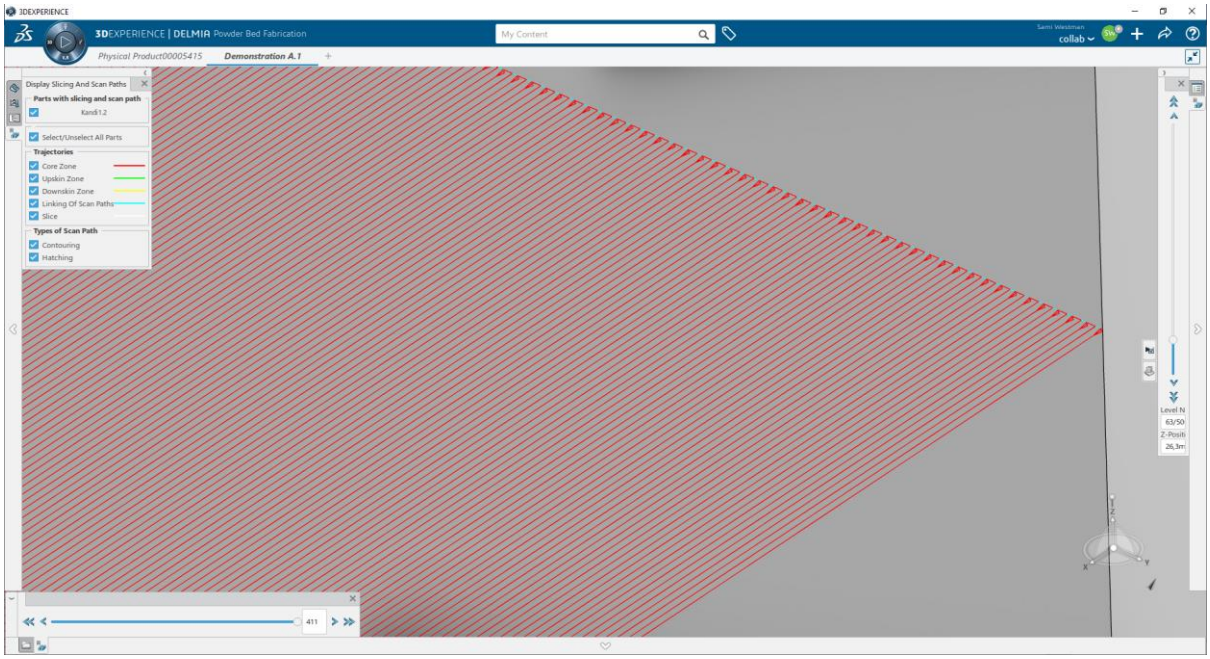

Figure 19. Illustration of scan path of laser beam on one layer in simulated part.

In figure 19, generated scan path of laser beam in part 1 can be seen. The software calculates and defines individual scan path for each layer that can be visualized.

4.2 Additive Manufacturing scenario App

A mesh is required for the simulation. Dividing the model into smaller pieces makes calculating distortions and stresses possible. Defining larger size mesh simplifies the simulation and shortens the simulation time but gets less accurate results. Used mesh type and sizes are listed on table 7.

Table 7. Meshing types and parameters used in simulation

Mesh	Type	Size [mm]	Thickness [mm]
Part	Linear partition hex	1	-
Support	Shell	1	1
Build platform	Sweep 3D	3	-

In table 7, the build platform mesh size can be three times larger than support and parts since results of the build platform do not need to be accurate. Linear partition hex is mesh build from cubes. Sweep 3D builds a mesh using rectangular cuboids. These elements are arranged as layers. Amount of these layers can be modified. Supports are only one element thick. Thickness of the supports can be defined by thickness of the mesh. After meshing the part, support and build platform need to be tied together.

Material used in the simulation is tool steel EOS MS1. Currently 3DExperience does not have AM metal materials in their database so manual definition of the used material is required.

Using thermo-mechanical analysis, the initial temperatures have to be defined for both models. Thermal model temperatures are set to chamber temperature for build platform, support and product, which is 300 K in this case. Mechanical model build platform is set to chamber temperature, but support and product temperatures are set to the relaxation temperature of the material. Relaxation temperature used is 800 K.

Moving heat flux is used to simulate the laser. Laser energy heats up the material. With absorption parameter simulation calculates how much of the laser energy the part absorbs. Convection coefficient and emissivity affects how fast the product cools down. Parameters are listed in table 8.

Table 8. Heat flux and cooling parameters.

Absorption	0.45
Convection coefficient [$\frac{W}{K*m^2}$]	18
Emissivity	0.25

Used absorption in this thesis is 0.45, as table 8 reveals. This means the part absorbs 45 % of the laser energy. Convection coefficient defines the thermal conductivity of the material. Emissivity means how much the material emits the heat from surface. These parameters are recommended by Dassault Systèmes.

Build platform is clamped in the structural analysis. This prevents the build platform from moving or deforming during the simulation. Rotational movement movement of supports are also locked to compensate for thinner supports. In thermal analysis a prescribed temperature is used to simulate heating of the build platform to 40 °C.

3DExperience is set to automatically collect data from each layer. One increment by layer. This usually gives too much data and makes simulation unnecessarily time consuming. In this simulation, data is collected in ten-layer increments.

5 RESULTS AND DISCUSSION

Results of the simulations are represented in this chapter. For every part there are four pictures which include von Mises stress full part, von Mises stress from inside, distortions and distortion vectors. From von Mises stresses at the surface of the part and inside the part can be seen. Distortion and distortion vectors show the amount and direction of distortions. Build platforms are left in the model to shorten the simulation time.

5.1 Overhang

Part 1 is overhang. Overhang should normally be made with supports but supports have been left out to maximize distortions. In figures 20-21 are shown von Mises stresses for part 1

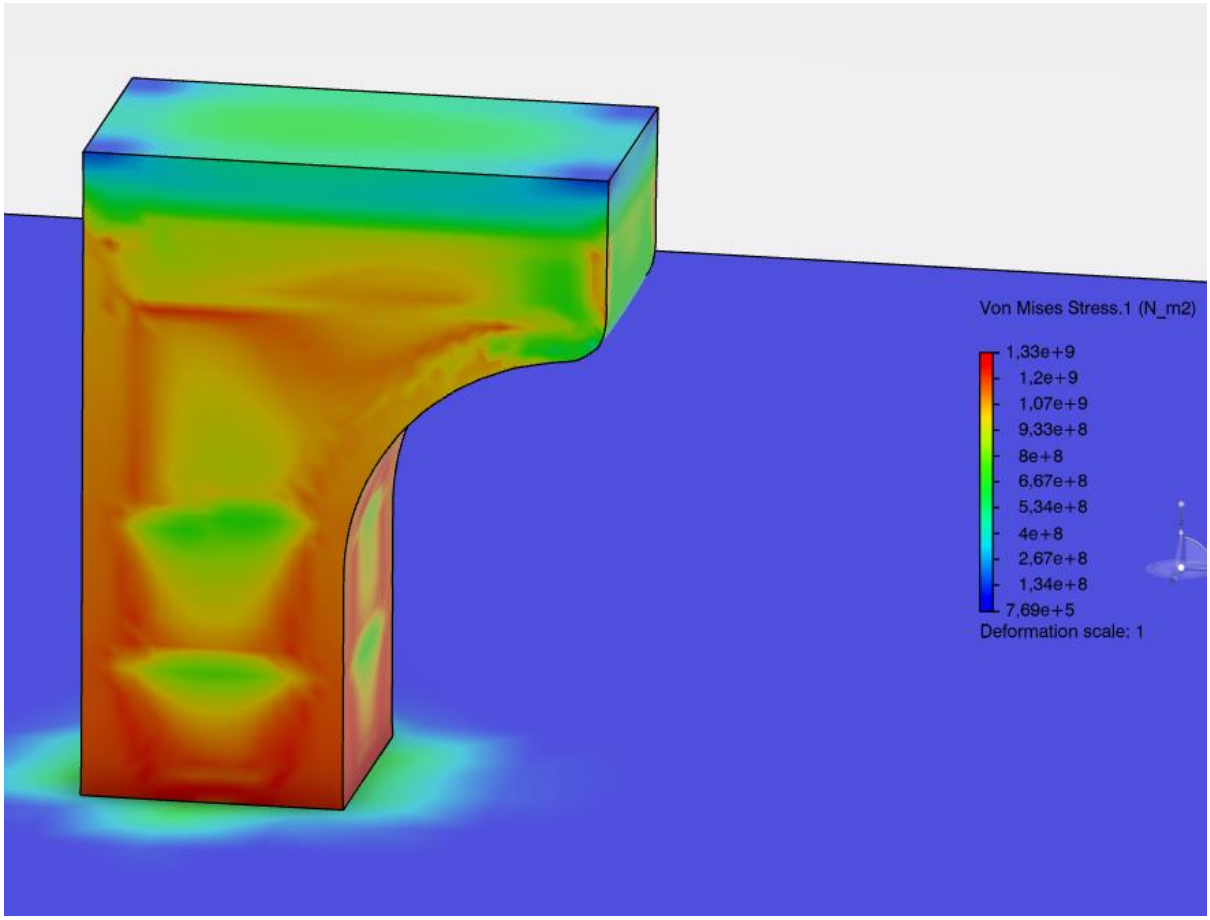

Figure 20. Von Mises stress results of part 1.

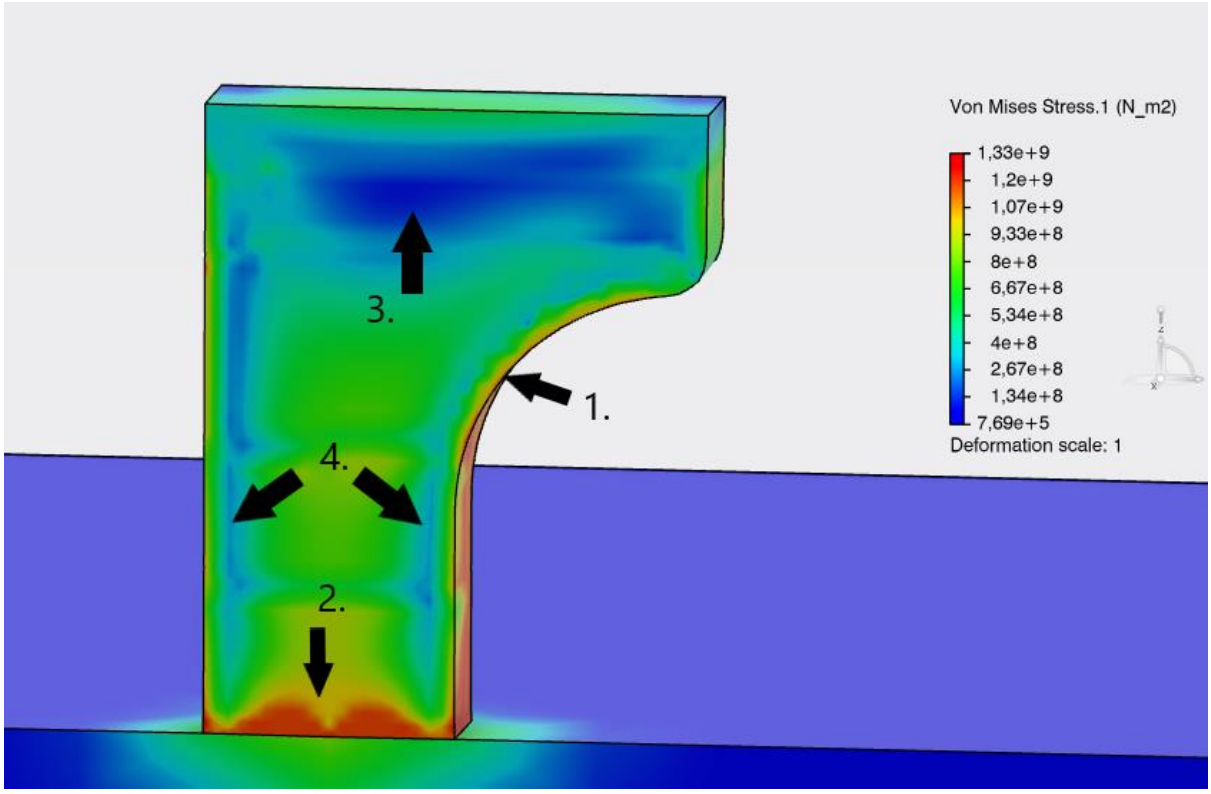

Figure 21. Von Mises results of part 1 cut.

Figure 21 reveals that at the stress value of 1.33 GPa, it can be seen that the residual stresses are quite high. Reason for this might be that von mises stresses are high in simulation but issue need further study. However, as seen in figure 21 (cut) most of these are concentrated on the surface (point 1). Highest stress is formed near the bottom of the part (point 2) creating stress to the build platform. Average stresses get lower at the upper part. Lower stresses can be seen under the surface (point 4) Lowest stresses appear inside the part at upper levels (point 3). In figure 22-23 are shown distortions in part 1.

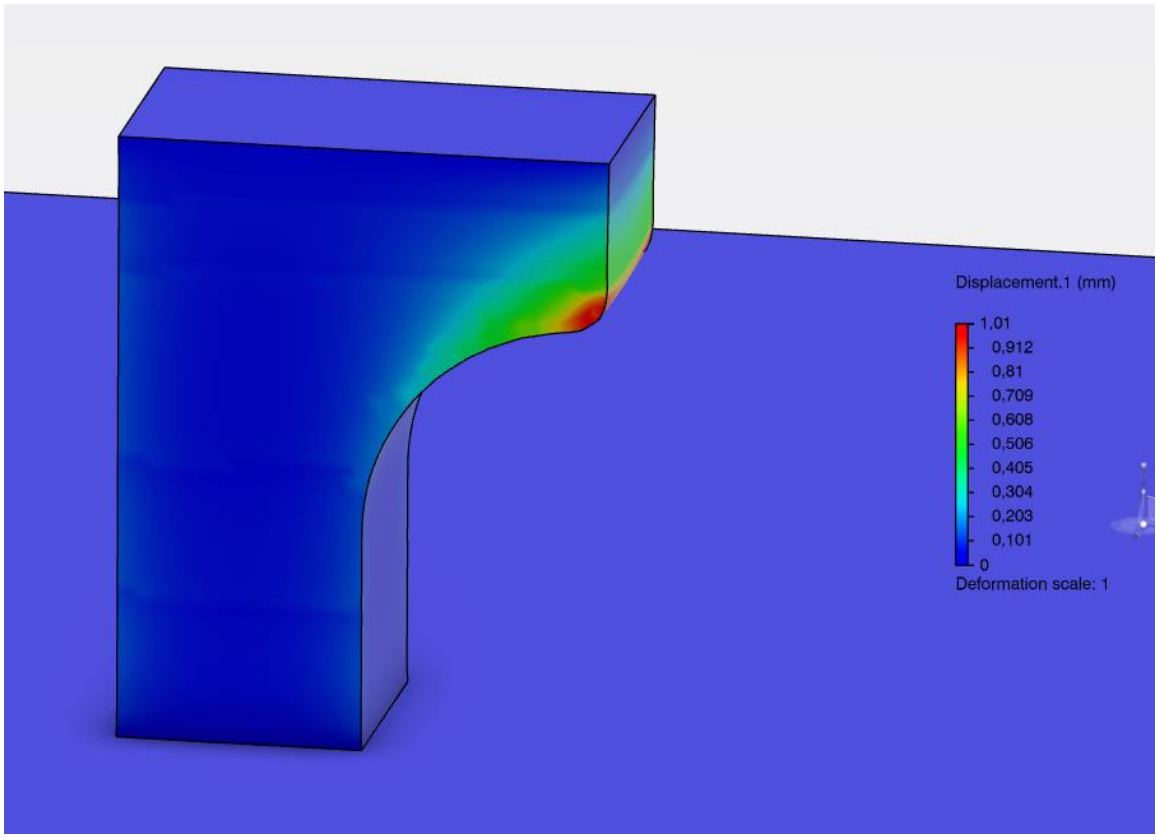

Figure 22. Displacement results of part 1.

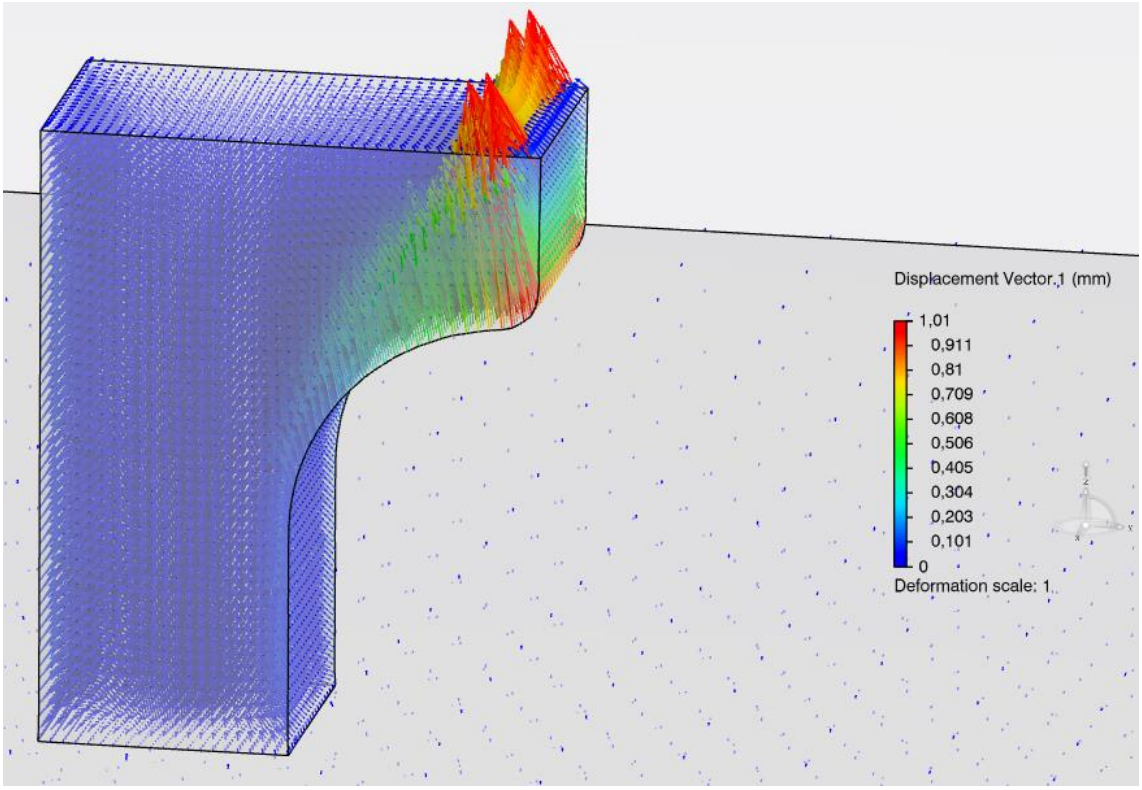

Figure 23. Displacement orientation vectors of part 1.

In figure 22 highest distortions are at the bottom of the overhang and they get larger when approaching the tip of the overhang. The overhang tries to bend upward especially from the corners as seen on figure 23. Distortion of 1 mm is huge in a part this small rendering it unusable. Distortion in the other parts are minimal and are all oriented inwards causing shrinkage.

5.2 Arch structure

Part 2 is arch structure. Part has been manufactured directly on build platform without supports. In figure 24-25 are shown stresses in part 2

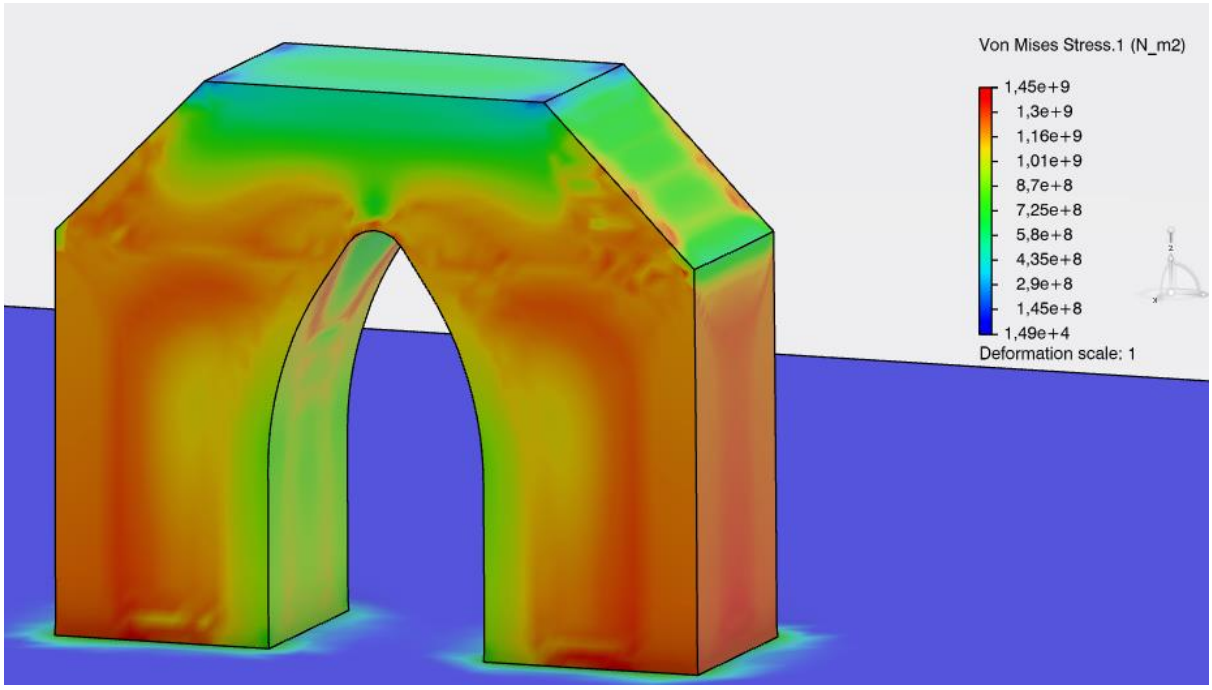

Figure 24. Von Mises stress results of part 2.

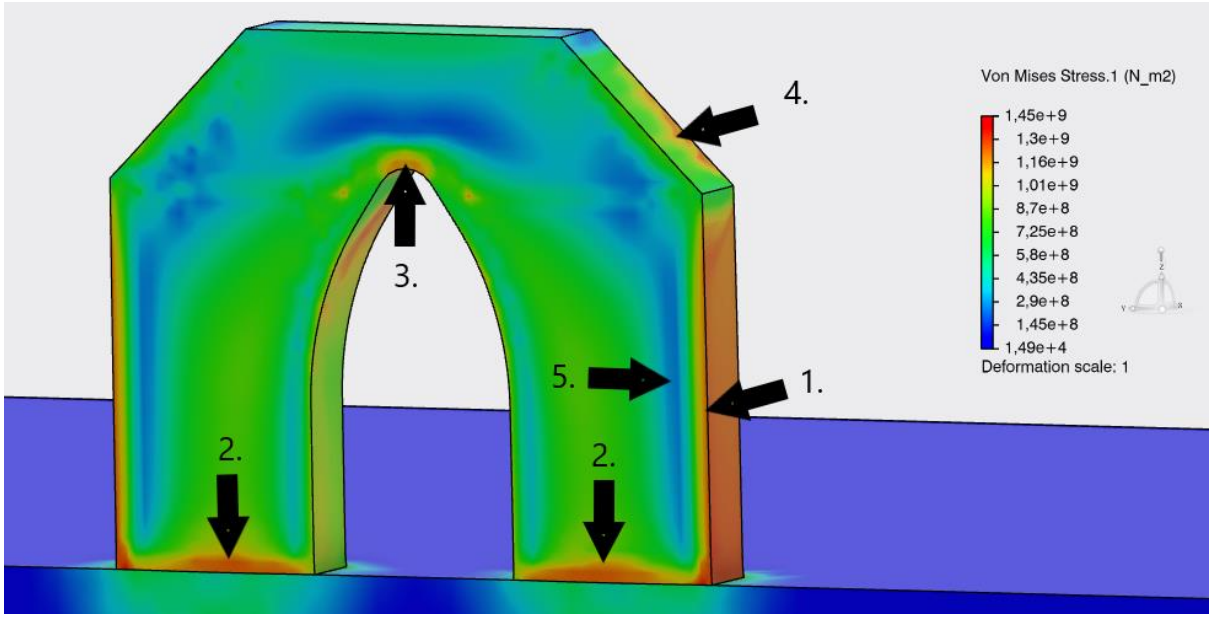

Figure 25. Von Mises stress results of part 2 cut.

In figures 24-25 stress concentration results are similar to part 1. The stresses are mostly concentrated on surfaces (point 1) and lower regions of the part (point 2). Stresses are higher at the highpoint of the arc (point 3) compared to part 1, where stresses were smaller at the tip of the overhang. At the angled outer surface are higher stresses at the point where the halves meet (point 4). Inside surface of the arch (near point 3) has a lot of smaller stresses with two lines from bottom to arch ceiling having higher stresses. Lowest stress on the inside (point 5) follows the geometry of the arch.

In figures 26-27 is shown the distortions and their orientation in part 2.

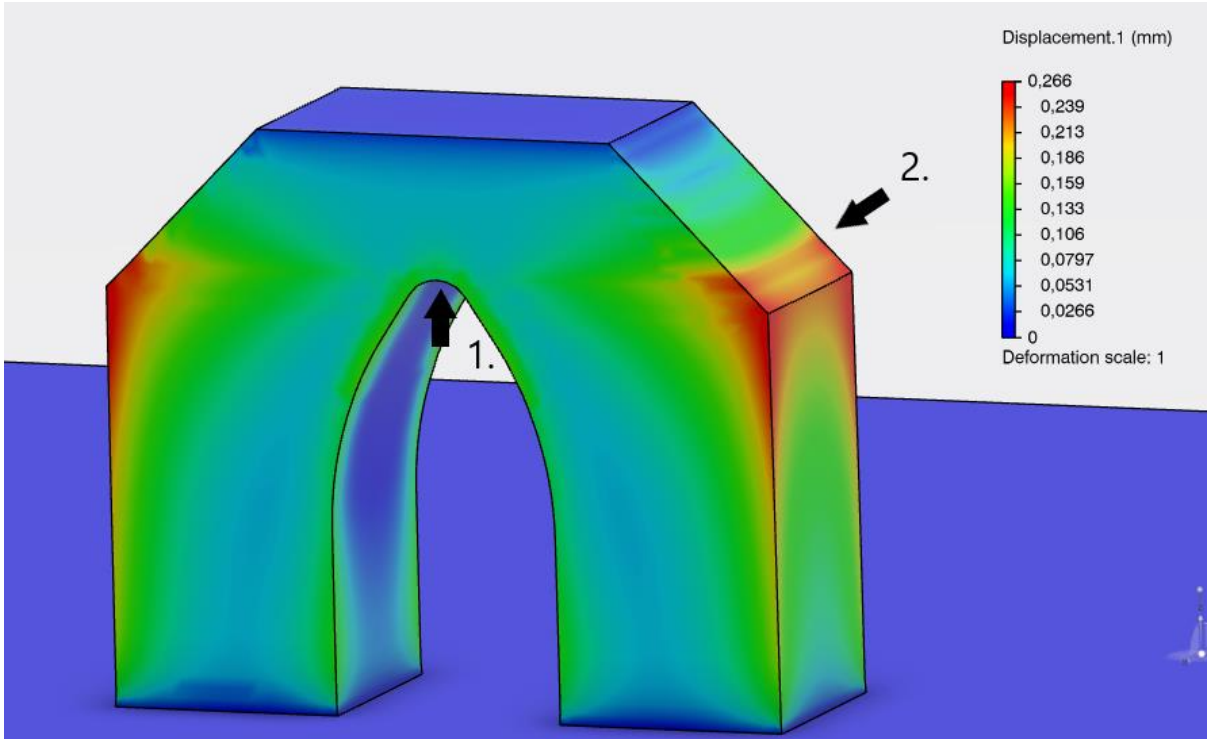

Figure 26. Displacement results of part 2

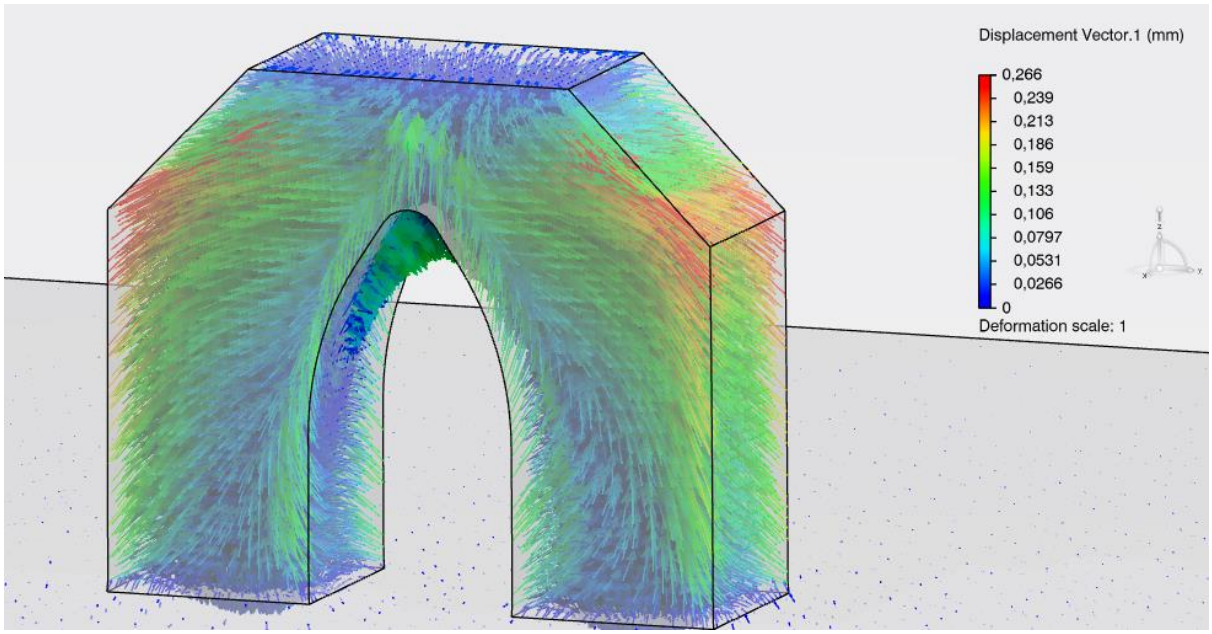

Figure 27. Displacement vectors of part 2

Distortions mostly range from close to zero to 0.16 mm in figures 26-27. However, at the outside surface is where the largest distortions appear. These distortions are mostly concentrated on edges at the arch unison height (point 2). Largest distortions cause the outer surface to have shrinkage grooves as in the study conducted by Kokkonen et al. Larger stresses under the arch (point 1) does not seem to have effects on distortion. Bottom of the part tries to distort through build platform. This could cause higher stresses appearing there.

5.3 Horizontal plate

Part 3 is horizontal plate with three plates on top of it. Plate has been manufactured on 5 mm tall supports. Figure 28 represents stresses in part 3.

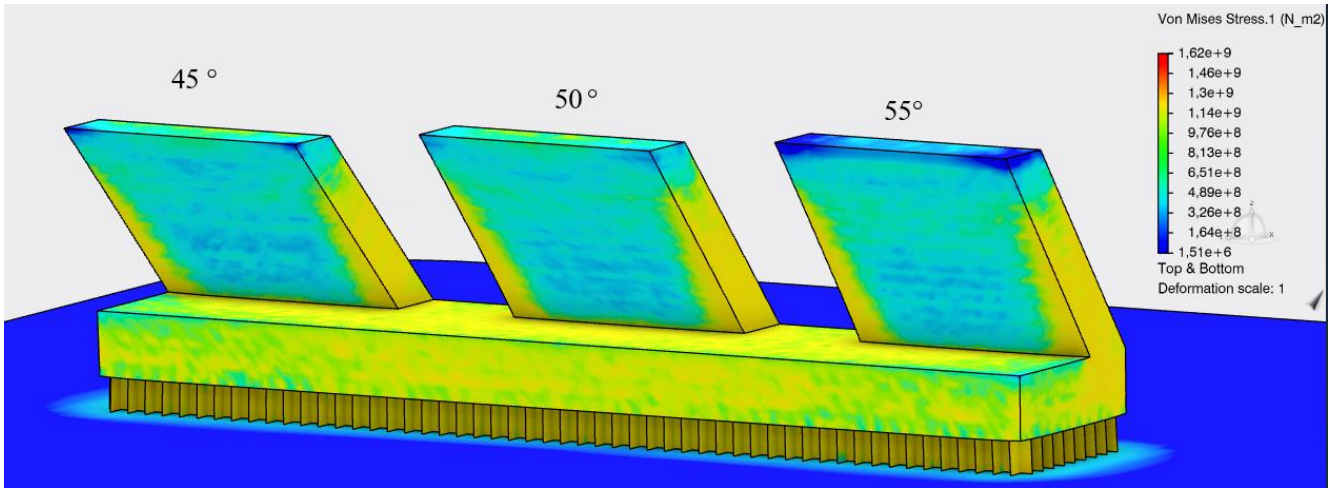

Figure 28. Von Mises results of part 3

Highest stresses shown in figure 28 are results of stresses in support structure which would be thicker in real print resulting in less stress. Highest stresses in the actual part are 1.23 GPa ($10^9 \cdot N/mm^2$). Same trend can be seen as in parts 1-2 where highest stresses tend to be on the side surfaces while insides and tops have less stress. Figures 29-30 shows deforming in part 3.

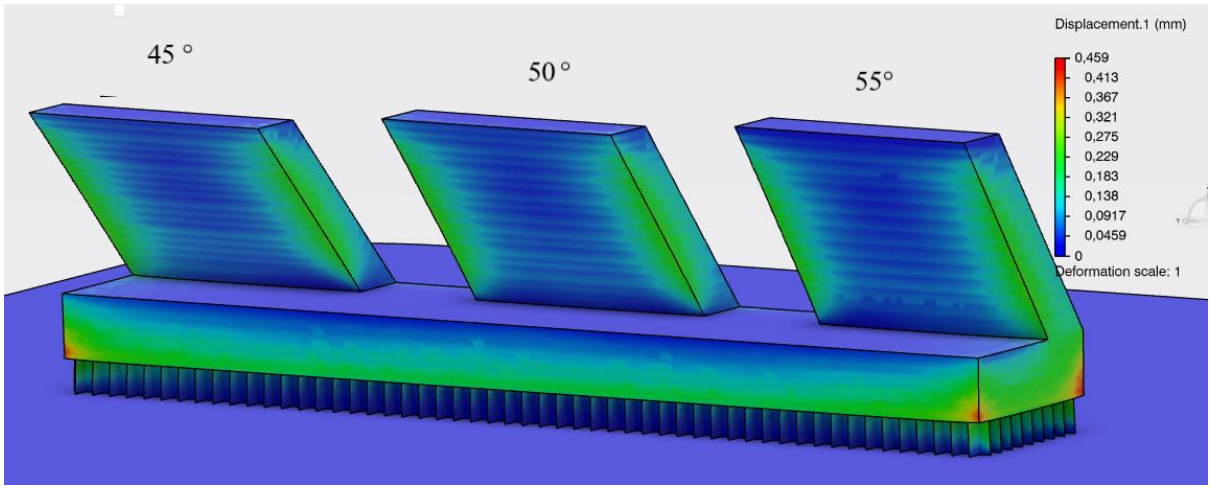

Figure 29. Displacement results of part 3.

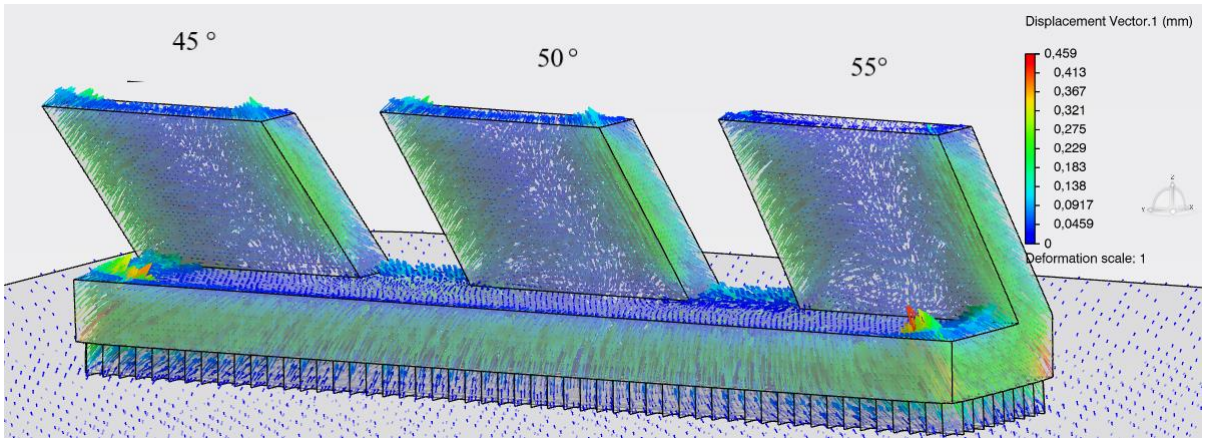

Figure 30. Displacement vectors of part 3.

In figure 29, part 3 deformation mostly occurs at bottom of the part and edges. In figure 30 it can be seen that vectors on the bottom plate are focused upwards and middle. If the part was cut from the support structures, it would bend upwards from both ends. The inclined plates are shrinking from sides, but amount is small enough not to be noticeable with naked eye. Same distortion as bottom plate cannot be seen on inclined plates.

5.4 Discussions

Highest stresses seem to form at the surfaces of the parts especially at the edges and at the bottom where part is connected to the build platform. These stresses exceed the yield strength of the MS1 causing the distortions. Distortion orientation trend can be seen to be inwards. This is most likely caused by contraction happening in melt pool when it cools down and

solidifies causing the whole part to shrink. Highest distortion can be seen in part 1. This distortion is about 1 mm which is a lot higher than distortion in part 2 even though part 2 has higher stresses. In part 2 the arch is supported from both sides. Part 1 overhang is not supported which allows it to distort freely. Using supports could reduce distortions. Stresses in part 3 were distributed more evenly. Distortions were concentrated in corners which lacks support from structure itself. It seems thin horizontal geometries has tendency to distort. Same distortions cannot be seen on inclined plates. Distortions could be avoided with orientation of the part.

6 CONCLUSIONS

Aim of this thesis is to characterize thermal effects of L-PBF on manufactured part, based on simulation. Characterization of deformations by simulation could save resources in test prints by optimizing AM process before first process. Thesis was conducted with literature review of simulation process and geometries. Experimental part was done with simulation on 3DExperience using thermo-mechanical method.

This study was carried out as part of Metal 3D Innovations (Me3DI) project funded by European Regional Development Fund (ERDF). Aim of this project is to form knowhow cluster for metal 3D printing to South Karelia. Project started 1.9.2018 and it ends 31.12.2020. Thesis was produced in Research Group of Laser Material Processing and Additive Manufacturing (3D Printing) of Department of Mechanical Engineering at LUT University

Simulated geometries were decided to be similar to test parts found in literature review. This was done to prevent the thesis from being too broad and to verify simulation results. 3DExperience platform was used to model and simulate the parts. Thermo-mechanical method was used for simulation. Used parameters were EOS M290 AM devices parameters for tool steel MS1.

Simulating AM process could help in manufacturing of multiple parts in the same process. This could save money and time but requires further studies

Material is melted in L-PBF with high energy laser. This temperature increase causes temperature expansion and contraction when it cools down. This thermal behavior creates distortions and residual stresses in the part. Prevention of this issue requires further studies.

In literature review, it was found that arch structures, overhangs and thin horizontal plates were problematic in AM. Archs and overhangs could be manufactured without support structures but it would cause heat buildup and allow increased freedom to distort.

Residual stresses formed mostly on the surface of the parts and at the interface of the part and build platform. Highest stresses were concentrated on corners. These stresses would often exceed yield strength of the material causing further distortions. Distortions formed on less supported parts. Highest distortions were encountered in thin unsupported horizontal structures. These distortions were smaller if structure was supported. On inclined structures these stresses were not seen. Stresses could be avoided with orientation of the part.

Printing overhangs without supports reduces print time and amount of material used. These reductions come at a cost. Supports also helps conducting heat better than raw powder. Better heat conduction decreases heat buildups. These heat buildups caused dross to form at the surface.

7 FURTHER STUDIES

It is possible to simulate build platform and support removal on 3DExperience. This would give more accurate results since removing them causes distortions and stresses to shift. Simulating heat treatment could give results on how much of the stresses and distortions are recoverable. Simulation used in thesis did not get results for surface quality. Further studies could be conducted to achieve this.

3DExperience has possibilities to gain other results than residual stress and distortions from simulation. Further studies of possible results could be useful.

Multiple methods exist to simulate 3D-printing process. In further studies these methods could be used and compared to each other to study the differences in results. Real print could also be made to study how close the simulation results are.

LIST OF REFERENCES

Acharya, R., Sharon, J. A. & Staroselsky, A. 2017. Prediction of microstructure in laser powder bed fusion process. *Acta Materialia, 124*, Pp. 360-371.

Amal, C., Elkaseer, A. & Scholz, S. 2020. Dimensional Errors Due to Overhanging Features in Laser Powder Bed Fusion Parts Made of Ti-6Al-4V. *Applied Sciences, 10*(7), p. 2416.

Bugatti, M. & Semeraro, Q, 2018, Limitations of the inherent strain method in simulating powder bed fusion process. Additive Manufacturing 23. Pp. 329-346

Cyr, E., Lloyd, A. & Mohammadi, M. 2018. Tension-compression asymmetry of additively manufactured Maraging steel. *Journal of Manufacturing Processes, 35*, pp. 289-294.

Dassault Systèmes. 2020. 3DExperience platform. [Dassault Systèmes webpage]. [Referred 6.6.2020] Available: https://www.3ds.com/about-3ds/3dexperience-platform/

Diegel, O., Nordin, A. & Motte, D. 2019. A Practical Guide to Design for Additive Manufacturing.Singapore: Springer. 226 p.

EOS M290. 2019. [web document]. (Publishing place unknown): EOS, 2019. [referred on 27.5.2020] available: https://www.eos.info/en/additive-manufacturing/3d-printing-metal/eos-metal-systems/eos-m-290

Gouge, M., Denlinger, E., Irwin, J., Li, C. & Michaleris, P. 2019. Experimental validation of thermo-mechanical part-scale modeling for laser powder bed fusion.Additive Manufacturing 29. Pp. 1-17.

Gouge, M. and Michaleris, P., 2018. *Thermo-mechanical modeling of additive manufacturing.* Kidlington, Oxford: Butterworth-Heinemann, an imprint of Elsevier.

Han, Q., Gu, H., Soe, S., Setchi, R., Lacan, F. & Hill, J. 2018. Manufacturability of AlSi10Mg overhang structures fabricated by laser powder bed fusion. *Materials & Design, 160*, pp. 1080-1095.

Kokkonen, P, Salonen, L, Virta, J, Hemming, B, Laukkanen, P, Savolainen, M, Komi, E, Junttila, J, Ruusuvuori, K, Varjus, S, Vaajoki, A, Kivi, S & Welling, J 2016, *Design guide for additive manufacturing of metal components by SLM process*. VTT Research Report, vol. VTT-R-03160-16, VTT Technical Research Centre of Finland.

Masoomi, M., Thompson, S. M. & Shamsaei, N. 2017. Laser powder bed fusion of Ti-6Al-4V parts: Thermal modeling and mechanical implications. *International Journal of Machine Tools and Manufacture, 118-119,* Pp. 73-90

Milewski, J.O. 2017. Additive Manufacturing of Metals. From Fundamental Technology to Rocket Nozzles, Medical Implants, and Custom Jewelry. Cham: Springer. 343 p

Neto, M. A., Amaro, A., Cirne, J., Leal, R. & Roseiro, L. 2015. *Engineering Computation of Structures: The Finite Element Method*. 1st ed. 2015. Cham: Springer International Publishing.

Peng, H., Ghasri-Khouzani, M., Gong, S., Attardo, R., Ostiguy, P., Gatrell, B. A., . . . Hoelzle, D. 2018. Fast prediction of thermal distortion in metal powder bed fusion additive manufacturing: Part 1, a thermal circuit network model. *Additive Manufacturing, 22,* Pp. 852-868.

Lou, S., Jiang, X., Sun, W., Zeng, W., Pagani, L. & Scott, P. 2019. Characterisation methods for powder bed fusion processed surface topography. *Precision Engineering, 57,* Pp. 1-15.

Wang, X. & Chou, K. 2018. Effect of support structures on Ti-6Al-4V overhang parts fabricated by powder bed fusion electron beam additive manufacturing. *Journal of Materials Processing Tech, 257,* p. 65-78.

Yaghi, A., Ayvar-Soberanis, S., Moturu, S., Bilkhu, R. & Afazov, S. 2019. Design against distortion for additive manufacturing. *Additive Manufacturing, 27,* pp. 224-235.

Yan, Z., Liu, W., Tang, Z., Liu, X., Zhang, N., Li, M. & Zhang, H. 2018. Review on thermal analysis in laser-based additive manufacturing. *Optics and Laser Technology, 106*, Pp. 427-441

Yang, Y., Jamshidinia, M., Boulware, P. & Kelly, S. 2018. Prediction of microstructure, residual stress, and deformation in laser powder bed fusion process. *Computational Mechanics, 61*(5), pp. 599-615

APPENDIX I, 1

Full list of parameters used for simulation

Property	Value
Max scan speed [mm/s]	7000
Max scan power [W]	400
Max jump speed [mm/s]	7000
Focal diameter [mm]	0,1
Maximal Defocusing Length [mm]	0,1
Shape type	Rectangle
Length [mm]	300
Width [mm]	300
x [mm]	0
y [mm]	0
z [mm]	200
Relaxation temperature [°C]	490
Heated build platform [°C]	40
Absorption	0,4
Convection coefficient [$\frac{W}{K*m^2}$]	18
Emissivity	0,25
Beam power [W]	285
Defocusing length [mm]	0
Jump Speed [m/s]	7
Delay after jump [s]	0
Scan speed [m/s]	0,96
No initialization	false
Product Mesh size [mm]	1
Support mesh size [mm]	1
Thickness [mm]	1
Build platform mesh size [mm]	3
Range	1

start	1
periodicity	1
Slicing step [mm]	0,1
Minimal skin width [mm]	1
Number of layers	1
Restrict core by Upskin	True
Pending time before recoating [s]	0
Recoating time [s]	0
Recoating break time [s]	9
Pending time after recoating [s]	0
Start temperature [K]	300
Gas inlet direction [°]	0
Gas flow [$\frac{m^3}{s}$]	0
Scanning iteration of first slice	1
Part order scanning	default
Order scan paths	part
Support first	False
Manufacturing orientation frozen	True
Distance between part and build platform [mm]	5
Distance between part and build platform	false
Minimum distance between parts [mm]	1
Clearance on build platform border [mm]	1
Minimum height between parts [mm]	1
Nesting options	Nesting 2D with bounding box of the part
Zone type	Zones as surfaces
Ground type	all
Minimal surface widht [mm]	5
Tolerance [mm]	0,01
Minimum surface angle [°]	0
Maximum surface angle [°]	45

Shape type	Wired support
Pattern	grid
With envelope	false
Spacing [mm]	3
Direction angle [°]	0